nature neuroscience

Separate circuitries encode the hedonic and nutritional values of sugar

Luis A Tellez[1,2], Wenfei Han[1,2], Xiaobing Zhang[3], Tatiana L Ferreira[1,2,4], Isaac O Perez[1], Sara J Shammah-Lagnado[5], Anthony N van den Pol[3] & Ivan E de Araujo[1,2,6]

Sugar exerts its potent reinforcing effects via both gustatory and post-ingestive pathways. It is, however, unknown whether sweetness and nutritional signals engage segregated brain networks to motivate ingestion. We found in mice that separate basal ganglia circuitries mediated the hedonic and nutritional actions of sugar. During sugar intake, suppressing hedonic value inhibited dopamine release in ventral, but not dorsal, striatum, whereas suppressing nutritional value inhibited dopamine release in dorsal, but not ventral, striatum. Consistently, cell-specific ablation of dopamine-excitable cells in dorsal, but not ventral, striatum inhibited sugar's ability to drive the ingestion of unpalatable solutions. Conversely, optogenetic stimulation of dopamine-excitable cells in dorsal, but not ventral, striatum substituted for sugar in its ability to drive the ingestion of unpalatable solutions. Our data indicate that sugar recruits a distributed dopamine-excitable striatal circuitry that acts to prioritize energy-seeking over taste quality.

Unlike artificial sweeteners, sugar promotes ingestive behavior via both gustatory and post-ingestive pathways[1–4]. However, the neural mechanisms mediating sugar's dual control over behavior remain elusive. Specifically, it remains unknown whether gustatory and post-ingestive signals recruit shared or segregated neural circuitries to promote intake. Overcoming our incomplete understanding of how calories modify the reward value of sweet substances should provide new strategies for curbing excess sugar intake[4].

In the vertebrate brain, the striatal areas of the basal ganglia are crucial for selecting reward-based actions and evaluating their outcome[5–8]. In the striatum, the anatomical segregation between dorsal and ventral regions is an evolutionarily conserved trait[9] previously linked to dissociable behavioral functions[6,10]. The execution of these anatomically specific behavioral functions critically depends, in turn, on striatal dopamine signaling[7,11,12]. We investigated whether the distinction between gustatory versus post-ingestive reward reflects the anatomical specialization between ventral versus dorsal dopamine-controlled striatal sectors.

RESULTS

Taste and nutrition separately control dopamine levels

We started by monitoring dopamine release in both ventral (VS) and dorsal (DS) striatal sectors during the active intake of nutritive and non-nutritive sweeteners. Briefly, mice licked a spout containing a non-caloric sweetener (sucralose), such that lick detection by the contact lickometer triggered intra-gastric infusions of solutions containing either sucralose or sugar (D-glucose). This procedure, performed concomitantly to brain microdialysis (**Supplementary Fig. 1a**,**b**), eliminates potential confounds associated with differences in taste quality/intensity between sugars and artificial sweeteners. We chose D-glucose to model sugar ingestion because of its unvarying presence in sugared products.

We observed increased dopamine release above baseline levels in VS during sweetener intake, irrespective of which solution was administered intra-gastrically (**Fig. 1a**). However, dopamine release in DS increased above baseline levels only when sweetener intake was accompanied by intra-gastric infusions of glucose (**Fig. 1b**), suggesting that DS-projecting dopamine cells are selectively sensitive to sugar. We assessed the effect on dopamine release produced by lessening the hedonic value of the solutions. We achieved this by adulterating the sucralose solution with the bitter compound denatonium benzoate. In these experiments, licking the sweet/bitter stimulus was always accompanied by intra-gastric infusions of glucose. Notably, although sweetener adulteration suppressed sugar-induced dopamine release in VS (which did not surpass baseline levels), evoked dopamine release remained similarly robust, rising above baseline levels in DS (**Fig. 1c** and **Supplementary Fig. 1c**,**d**). Note that sugar-induced changes in dopamine levels failed to rise above baseline levels in VS despite the energy content of the solutions. Thus, although energy *per se* is capable of driving dopamine release in VS[3,13], taste quality gates this sugar-induced ventral dopamine efflux[14,15].

We then performed the reciprocal experiment by replacing D-glucose with its non-metabolizable enantiomer L-glucose. In these experiments, licking the sweet stimulus was accompanied by intra-gastric infusions of the non-metabolizable sugar. In marked symmetry with the previous experiment, whereas replacing D-glucose with L-glucose suppressed

[1]The John B. Pierce Laboratory, New Haven, Connecticut, USA. [2]Department of Psychiatry, Yale University School of Medicine, New Haven, Connecticut, USA. [3]Department of Neurosurgery, Yale University School of Medicine, New Haven, Connecticut, USA. [4]Mathematics, Computing and Cognition Center, Federal University of ABC, Santo André SP, Brazil. [5]Department of Physiology and Biophysics, Biomedical Sciences Institute, University of São Paulo, São Paulo SP, Brazil. [6]Department of Physiology, Yale University School of Arts and Sciences, New Haven, Connecticut, USA. Correspondence should be addressed to I.E.d.A. (iaraujo@jbpierce.org).

Received 23 October 2015; accepted 3 December 2015; published online 25 January 2016; doi:10.1038/nn.4224

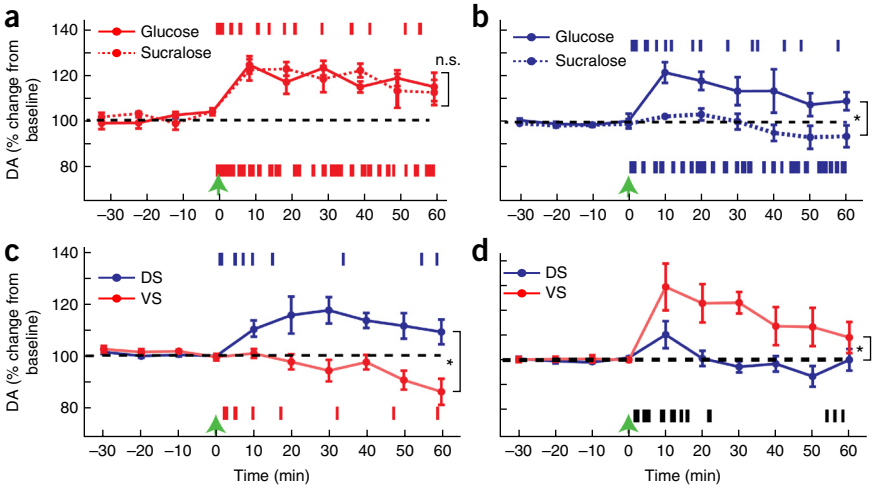

Figure 1 Gustatory and nutritional signals separately control dopamine levels in ventral versus dorsal striatum. (**a**) Higher ventral striatal DA levels were observed during sucralose licking following intra-gastric infusions of both glucose ($N = 6$) and sucralose ($N = 6$, two-way mixed model ANOVA, sucralose versus glucose effect $F[1,4] = 0.006$, $P = 0.94$). Graph displays changes in DA during the 1-h intake session after 30 min of baseline sampling. Raster plot shows across-animals average lick rates for each (sucralose versus glucose) session type, with total lick counts shown in 10-min bins. Onset of licking is shown by green arrow. Sessions involving sucralose infusions are shown as dotted lines, and sessions involving glucose infusions as solid lines. For comparisons against baseline, see **Supplementary Figure 1**. (**b**) Higher dorsal striatal DA levels were observed following intra-gastric infusions of glucose ($N = 6$) compared with sucralose ($N = 6$, $F[1,10] = 8.2$, $^*P = 0.017$). Note that DA levels following sucralose infusions remained at baseline levels (represented by horizontal dotted line). (**c**) Adulteration of the sucralose solution with bitter compound inhibited DA release in VS ($n = 7$), but not DS ($n = 8$, two-way mixed effects ANOVA, DS versus VS effect $F[1,13] = 15.7$, $^*P = 0.002$). All animals received D-glucose intra-gastric infusions following licking. (**d**) Intra-gastric infusions of non-metabolizable L-glucose inhibited sugar-induced dopamine release in DS, but not VS ($n = 6$, two-way within-subjects ANOVA, DS versus VS effect $F[1,5] = 13.9$, $^*P = 0.013$). VS and DS were sampled simultaneously (licks shown in one raster, dark). n.s., not statistically significant. Error bars represent s.e.m.

sugar-induced dopamine release in DS (which did not surpass baseline levels), sweetness-induced dopamine release remained similarly robust, rising above baseline levels in VS (**Fig. 1d** and **Supplementary Fig. 1e**,**f**). Notably, the observed sugar-induced changes in dopamine levels were not associated with licking rates *per se* (**Supplementary Fig. 1g**,**h**). In fact, intra-gastric infusions performed outside any behavioral context (that is, in the absence of licking activity) produced sugar-induced increases in dopamine levels that were statistically indistinguishable from those observed during the behavioral sessions (glucose DS (behavioral sessions, $N = 6$; passive infusions, $N = 5$): group effect $F[1,9] = 0.02$, $P = 0.89$; **Supplementary Fig. 1i**,**j**). Furthermore, sugar-induced dopamine release did not require intra-gastric glucose to be a novel stimulus, nor did it evoke unspecific motoric activities (**Supplementary Fig. 2**). In sum, whereas taste quality regulates dopamine release in ventral striatum, increases in dopamine release in dorsal striatum are under strict metabolic control.

Increasing dopamine levels mimics taste and nutrition

We next analyzed the functional implications of metabolism-driven dopamine release in DS. We found that hungry mice consume significantly more of the unpalatable solution when associated with intra-gastric sugar compared to intra-gastric artificial sweetener (paired t test, $t[7] = 2.62$, $P = 0.035$; **Supplementary Fig. 3a**,**b**). Consistent with a role for DS dopamine signaling in this phenomenon[6,10,11], perfusion of either VS or DS with dopamine via reverse microdialysis induced robust licking of the unpalatable solution (**Supplementary Fig. 3c**,**d**). In sum, hungry mice endure unpalatable solutions when those are associated with gut energy sensing, an effect mirrored by artificially increasing extracellular dopamine levels in DS and VS (thereby mimicking the effects of nutrition and sweetness on dopamine release).

D1r neurones in DS drive nutrient seeking

We next tested whether striatal dopamine signaling mediates the functional organization of basal ganglia pathways in terms of hedonics versus nutrition. Given that dopamine increases the excitability of D1r-expressing neurones[16,17], we specifically focused on their role in sugar reward. We first performed loss-of-function cell ablation studies. We achieved cell-specific ablation of D1r-neurones in DS or VS by virally introducing a Cre-dependent caspase into D1r-Cre mice. Specifically, the Cre-dependent viral construct AAV-flex-taCasp3-TEVp[18] was stereotaxically injected bilaterally into DS or VS of D1r-Cre mice. Non-Cre mice transfected with AAV-flex-taCasp3-TEVp were used as controls.

We first assessed the effect of cell-specific ablations on taste responses by employing brief-access licking tests[19]. Test stimuli consisted of a sucralose solution mixed to increasing levels of the bittering agent denatonium. We found that ventrally ablated (VS-casp) mice were significantly more affected by the lowest concentrations of denatonium, whereas dorsally ablated (DS-casp) mice were similar to controls (WT-casp; two-way RM-ANOVA, bitterness × lesion site $F[6,57] = 3.38$, $P = 0.006$; group effect $F[2,16] = 3.59$, $P = 0.048$; **Fig. 2a**). Similar results were obtained when increasing concentrations of sweetener were used to mask bitterness (**Supplementary Fig. 3e**). We then performed the converse experiment by presenting mice with a fixed bitter solution and pairing licks to increasing concentrations of intra-gastric glucose. When the concentration of the glucose infusate was low, VS-casp mice were again significantly more affected by bitterness than DS-casp and WT-casp mice (one-way ANOVA group effect $F[2,21] = 7.07$, $P = 0.005$; VS-casp versus DS-casp (Bonferroni-corrected $P = 0.023$) and WT-casp (Bonferroni-corrected $P = 0.007$); **Fig. 2b**). When the concentration of the glucose infusate was increased, both VS-casp and WT-casp control mice markedly increased responding only to reach similarly high levels; however, DS-casp mice failed to do so, remaining at their baseline levels (**Fig. 2b** and **Supplementary Fig. 3f**). The lesion-specific differences then diminish following infusions of more satiating intra-gastric loads (**Supplementary Fig. 3f**).

We inquired whether the above phenomena generalizes to learned chemosensory cues by employing a taste-nutrient learning procedure[1,2]. Naive DS-casp, VS-casp and WT-casp mice were initially tested on brief-access two-bottle preferences involving a sucralose solution and an unpalatable bitter/sweet mixture. Not surprisingly, all mice preferred to lick the sweet-only solution (**Fig. 2c**). Next, mice were exposed to one-bottle learning sessions in which licks for the sweet solution were paired to intra-gastric infusions of the non-nutritive sweetener.

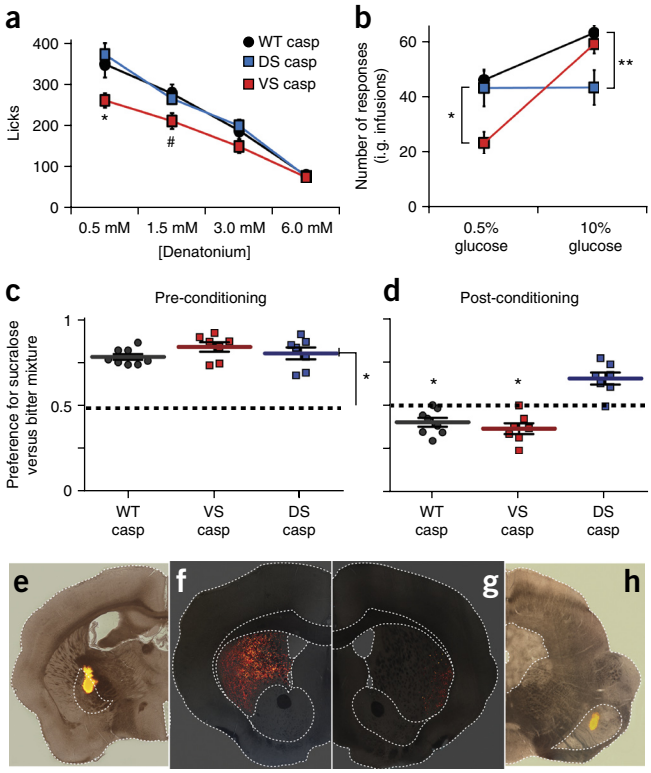

Figure 2 Cell-specific ablation of D1r neurones in DS, but not in VS, is necessary for sugar-driven consumption of unpalatable solutions. (**a**) Cell-specific ablation of D1r neurones in VS, but not in DS, increased the sensitivity to unpalatable solutions (two-way RM-ANOVA, bitterness × lesion site $F[6,57] = 3.38$, $P = 0.006$; group effect $F[2,16] = 3.59$, $P = 0.048$). VS-casp mice were particularly sensitive to the lower concentrations of bitter (one-way ANOVA main effect of lesion $F[2,21] = 6.19$, $P = 0.008$; VS-casp versus DS-casp (Bonferroni-corrected $^{*}P = 0.013$) or WT-casp control (Bonferroni-corrected $^{*}P = 0.029$ and $^{\#}P = 0.036$) groups. (**b**) Cell-specific ablation of D1r neurones in DS, but not VS, abolished sugar-induced consumption of unpalatable solutions (two-way RM-ANOVA, glucose concentration × lesion site effect $F[2,19] = 11.2$, $P = 0.001$; lesion site effect $F[2,19] = 4.4$, $P = 0.027$; glucose concentration effect $F[1,19] = 32.12$, $P = 0.000018$). Note that in the non-nutritive (0.5% glucose) condition ventrally lesioned VS-casp mice were more sensitive to bitterness than both control WT-casp and dorsally lesioned DS-casp mice (one-way ANOVA group effect $F[2,21] = 7.07$, $P = 0.005$; VS-casp versus DS-casp (Bonferroni-corrected $^{*}P = 0.023$) and WT-casp (Bonferroni-corrected $^{*}P = 0.007$). This effect was completely reversed by increasing the glucose concentration to nutritive levels, such that DS-casp mice failed to display similar increases in responding (one-way ANOVA group effect $F[2,21] = 7.09$, $P = 0.005$; DS-casp versus VS-casp (Bonferroni-corrected $^{**}P = 0.024$) and WT-casp (Bonferroni-corrected $^{**}P = 0.007$). (**c**) Taste-nutrient learning. Three groups of sugar/sweet naive, food-restricted mice (WT-casp, $N = 8$; DS-casp, $N = 7$; VS-casp, $N = 7$) were exposed to short-access 5-min two-bottle test between sucralose and an adulterated bitter/sucralose mix. As expected, all groups strongly preferred sucralose to the bitter mix (one-sample t tests against indifference ratio of 0.5, marked as horizontal dotted line: WT-casp, $^{*}P = 0.0000012$; DS-casp, $^{*}P = 0.00026$; VS-casp, $^{*}P = 0.000042$). (**d**) Next, the animals were exposed to 1-h conditioning one-bottle sessions where intake of the bitter mixture was paired to intra-gastric infusions of D-glucose, and intake of sucralose was paired to intra-gastric infusions of sucralose. Following the conditioning sessions, although WT-casp (Bonferroni-corrected $^{*}P = 0.036$) and VS-casp (Bonferroni-corrected $^{*}P = 0.045$) mice shifted preferences away from sweetness toward the nutritive bitter taste, DS-casp mice failed to shift preferences in response to gut glucose sensing (preference for sucralose > bitter mix, $P = 0.074$). (**e**–**h**) When Retrobeads were injected into globus pallidus (GP, dotted line in **e**, targeted by D2r-expressing neurons of DS) of DS-casp mice, strong labeling was observed throughout DS (**f**). In contrast, weak labeling was observed in DS (**g**) when Retrobeads were injected into SNr, on the opposite hemisphere to the one receiving a Retrobeads deposit in GP (dotted line in **h**). SNr is exclusively targeted by D1r-expressing neurons of DS. The same fluorescence (or lack thereof) pattern was observed in all animals sustaining the same injections. DS-casp: caspase-driven D1r-dependent lesions in DS of D1r-Cre mice ($N = 7$); VS-casp, caspase-driven D1r-depedent lesions in VS of D1r-Cre mice ($N = 7$); WT-casp, viral delivery of Cre-dependent caspase in DS and/or VS of non-Cre mice ($N = 8$). n.s., not statistically significant. Error bars represent s.e.m.

Then, on a different day, licks for the bitter/sweet solution were paired to intra-gastric infusions of the nutritive glucose. Two-bottle preference tests were performed again on a fourth testing day. All mice markedly shifted preferences toward the unpalatable nutritive stimulus, except DS-casp mice, which continued to prefer the non-nutritive, but palatable, solution (**Fig. 2d**). In sum, VS and DS D1r-neurone populations separately mediate the gustatory and nutritional actions of sugar. Notably, the lesions affected neither licking rates nor the amounts of intra-gastric sugar infused during conditioning (**Supplementary Fig. 3g**). Neuroanatomical criteria were employed to verify the specificity of the lesions (**Fig. 2e**–**h** and **Supplementary Fig. 3h**–**k**).

Activating D1r neurones in dorsal striatum mimics sugar

We further explored the circuit basis of the above phenomena by performing optogenetic gain-of-function studies. Using slice electrophysiological recordings, we confirmed increased excitability of mouse D1r-expressing neurones in the presence of dopamine (**Fig. 3a**,**b**). We thus tested the hypothesis that artificial activation of D1r-neurones in DS would substitute for sugar during ingestion of unpalatable adulterated sweeteners. Specific expression of the light-sensitive channelrhodopsin (ChR2) in D1r-neurones was achieved by stereotaxically injecting the Cre-dependent viral construct AAV-EF1a-DIO-hChR2(H134R)-EYFP into the VS and DS of D1r-Cre mice[20,21]. Slice electrophysiological recordings confirmed robust excitation of D1r-neurones by 473-nm laser pulses (**Fig. 3c** and **Supplementary Fig. 4**). Cre-dependent expression of ChR2 was confirmed by neuroanatomical criteria (**Fig. 3d** and **Supplementary Fig. 5a**,**b**).

During optogenetic experiments, mice licked a spout containing sucralose such that detected licks triggered light pulses to VS or DS, rather than intra-gastric infusions. Although optogenetic stimulation of D1r-neurones in VS significantly enhanced sucralose licking (paired t test, $t[5] = 5.63$, $P = 0.002$), it failed to attenuate the suppressive effects produced by adulterating sucralose with denatonium (**Fig. 3e**). The ability of VS stimulation to drive intake therefore depends on the hedonic properties of the stimulus and suggests the involvement of alternative circuits in intake suppression. However, stimulation of D1r-neurones in DS not only increased intake of sucralose, but also completely annulled the suppressive effects produced by the bitter toxin (**Fig. 3f** and **Supplementary Movie 1**). Notably, this was not a result of altered taste perception following light activation (**Supplementary Fig. 6a**) or of ceiling effects (**Supplementary Fig. 6b**–**e**). Optical activation induced self-stimulation (**Supplementary Fig. 6f**–**h**), but did not increase locomotor activity (**Supplementary Fig. 6i**). Moreover, optical activation did not alter the animals' sensitivity to either satiety or aversive sensory stimuli (**Supplementary Fig. 6j**,**k**). These data suggest that optical stimulation did not disrupt goal-direct action by inducing unspecific insensitivity to devaluation. In sum, D1r-neurone stimulation in DS, but not VS, substituted for sugar in its ability to drive ingestion of unpalatable stimuli.

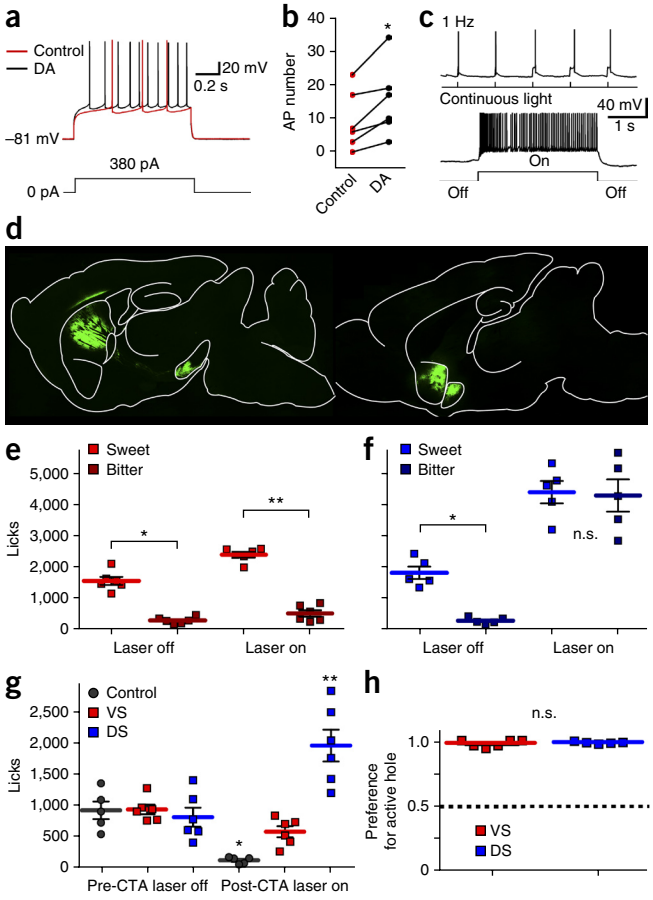

Figure 3 Optogenetic stimulation of D1r neurones in DS, but not in VS, substitutes for sugar in driving consumption of unpalatable solutions. (**a**) Representative traces showing DS D1r-neurone firing as evoked by a depolarizing current injection (380 pA, 1 s) in the presence of dopamine (30 μM, black) and control (shown in red) solutions. (**b**) Mean action potential (AP) counts during 1-s depolarization in the presence of dopamine and control solutions ($N = 6$, paired t test, $^*P = 0.013$). (**c**) Optogenetic activation of a ChR2$^+$ D1r neurone by 1-Hz blue light pulses (10 ms) and by a continuous light train (see additional analyses in **Supplementary Fig. 4**). This experiment was successfully replicated in ten cells sampled from two mice. (**d**) EYFP visualization confirmed that ChR2 transfection was contained to VS and DS. Note the dense bundles of axon terminals in VP and SNr, respectively. Images are composites of sequential 10× images of one entire sagittal section. The same fluorescence pattern was observed in all six animals sustaining the same injections. (**e**) In animals transfected with ChR2 in VS, adulteration of the sucralose solution by the bitter toxin produced a marked decrease in intake (laser OFF, $N = 6$, paired t test sweet versus bitter $t[5] = 10.03$, $^*P = 0.0002$) that was not reversed by D1r-neurone optogenetic stimulation (laser ON, $t[5] = 10.5$, $^{**}P = 0.0001$). (**f**) In animals transfected with ChR2 in DS, adulteration of the sucralose solution produced a marked decrease in intake (laser OFF, $N = 5$, $t[4] = 7.24$, $^*P = 0.002$) that was nevertheless totally reversed by D1r-neurone optogenetic stimulation (laser ON, $t[4] = 0.28$, $P = 0.79$). (**g**) Conditioned sweet taste aversion (CTA) induced by visceral malaise decreased intake in control (ChR2$^-$) mice (sweetener intake pre- versus post-malaise, $N = 5$, paired t test $t[4] = 5.76$, Bonferroni $^*P = 0.01$). Mice transfected with ChR2 in VS failed to increase intake despite laser stimulation ($N = 6$, $t[5] = 2.7$, Bonferroni $P = 0.1$). However, laser stimulation of DS markedly increased intake despite conditioned aversion ($N = 6$, $t[5] = 4.5$, Bonferroni $^{**}P = 0.01$). Overall group effect $F[2,14] = 13.1$, $P = 0.001$. (**h**) Optogenetic self-stimulation of VS and DS, as triggered by nose pokes (in the absence of food cues) produced equal numbers of pokes in the active versus inactive holes (ratio between pokes in active versus inactive holes is shown, DS ($N = 5$) versus VS ($N = 6$) effect $t[9] = 0.76$, $P = 0.47$). Error bars represent s.e.m. n.s., not statistically significant.

In addition, using a conditioned taste aversion procedure, we found that DS, but not VS, D1r-neurone stimulation overrode unpalatability produced by associating a novel sweetener (Rebaudioside A) to visceral malaise (**Fig. 3g**). Thus, unpalatability resulting from either innate bitterness or learned sickness is consistently overridden by DS stimulation. Notably, such disparities in VS and DS response patterns appeared to be limited to contexts associated with food intake: using a nose-poke-based protocol[20], we found equally potent D1r-neurone self-stimulation in both regions (**Fig. 3h**).

In addition to increasing excitability of striatal D1r neurones, dopamine concomitantly diminishes excitability of D2r neurones[16,17]. In fact, D2r neurones cooperate with D1r neurones to control goal-directed actions[22] and have a critical role in compulsive eating[23]. We therefore investigated the effects of optogenetically inhibiting D2r neurones on the intake of both the sweet and adulterated solutions. Inhibition of D2r neurones in VS slightly enhanced licking of the sweet solution without attenuating the aversive effects of adulteration by bitterness (**Supplementary Fig. 5c**). Inhibition of D2r neurones in DS, in contrast, did not affect licking of sweet solutions and only slightly attenuated adulteration effects (**Supplementary Fig. 5d**). Thus, unlike the case of D1r-neurone stimulation, unpalatability was not fully overridden by D2r-neurone inhibition. We note, however, that the above does not rule out an important role for D2r neurones in controlling sugar ingestion. Future experiments will need to determine the effects on intake of ablating D2r neurones in striatum.

D1r neurones in dorsal striatum override taste aversion

The major projections of DS D1r neurones are to the entopeduncular nucleus and the pars reticulata of substantia nigra (SNr). Because SNr is preferentially responsive to oral-facial movements[24], this target was chosen for optic and chemogenetic manipulations. In contrast, a major outflow of VS D1r neurones is directed to the ventral pallidum (VP). These DS and VS D1r targets are consistent with ChR2 terminal labeling (**Fig. 3d**). Given that DS and VS D1r neurones are GABAergic[7,9], the net outcome of stimulating D1r-striatal neurones is the inhibition of their downstream targets[25]. We therefore reasoned that optogenetic activation of SNr and VP would counteract the effects of stimulating DS and VS, respectively.

Consistent with an inhibitory tone exerted by VS and DS on VP and SNr, respectively, optogenetic activation of VP indiscriminately suppressed sweet intake, whereas the inhibitory effects produced SNr activation were gated by the presence of sugar in gut (**Supplementary Fig. 7**). These results provide initial support for the concept that sugar stimulation of dorsal pathways drives intake independently of the dopaminergic state of ventral pathways.

We explicitly tested the hypothesis that the dorsal DS → SNr pathway controls sugar intake independently of the sweetness-sensitive VS → VP ventral pathway. We employed a combination of optogenetics and chemogenetics[26]. One group of animals was ChR2 transfected in VS, and optical fibers were placed immediately above the D1r-neurone terminals in VP. A second group of animals was ChR2 transfected in DS, and optical fibers were placed immediately above the D1r-neurone terminals in SNr. To reversibly increase activity levels in the ventral output station, we stereotaxically injected animals in both groups with the construct AAV-hSyn-HA-hM3D(Gq)-IRES-mCitrine in VP (**Supplementary Fig. 8**).

In vivo neuronal activation and slice electrophysiology measures confirmed that D1r-positive VS terminals inhibited their VP targets

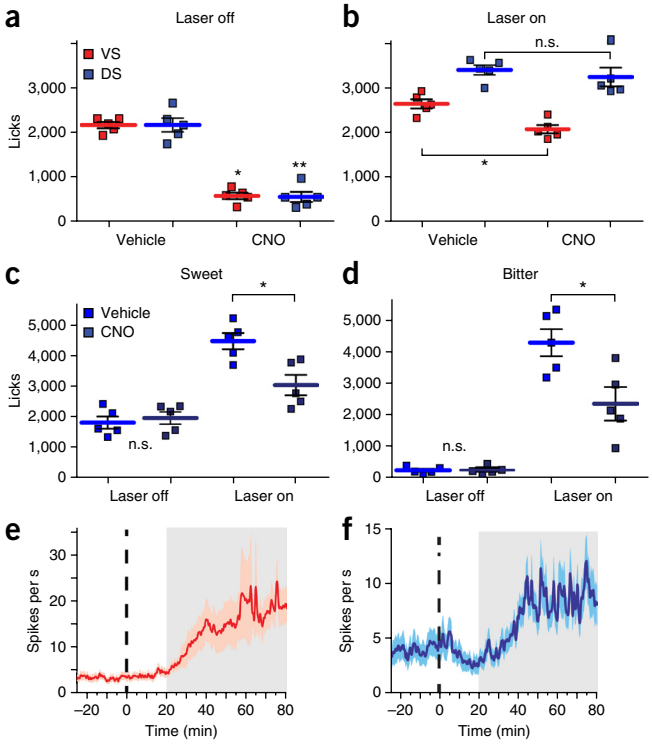

Figure 4 The dorsal striato-nigral pathway overrides inhibitory signals released by ventral output regions. We employed a combination of optogenetics and DREADDS. Animals expressed the designer receptor hM3D(Gq) in either VP or SNr (DREADD denoted by syringes in relevant locations, see scheme in **Supplementary Fig. 8**). One group of animals (VS → VP pathway) was ChR2 transfected in VS, and optical fibers were placed immediately above the D1r-neurone terminals in VP ($N = 5$). A second group of animals (DS→ SNr pathway) was ChR2 transfected in DS, and optical fibers were placed immediately above the D1r-neurone terminals in SNr ($N = 5$). (**a**) In the absence of light pulses, CNO administration robustly suppressed sweetener intake in both groups (VS → VP group, CNO versus saline effect paired t test $t[4] = 14.54$, Bonferroni $^*P = 0.00052$; DS → SNr group, $t[4] = 8.45$, $^{**}P = 0.004$). (**b**) Optogenetic activation of VS → VP terminals produced an increase in sweetener intake that was annulled by activating VP with CNO ($t[4] = 5.37$, Bonferroni $^*P = 0.024$). However, activating VP with CNO produced no effects on the robust increases in sweetener intake associated with optogenetically activating DS → SNr terminals ($t[4] = 0.98$, $P = 0.38$). (**c**) To assess pathway specificity, in an additional group of animals, we expressed hM3D(Gq) in SNr instead of VP. ChR2 was transfected in DS, and optical fibers were placed immediately above the D1r-neurone terminals in SNr. Optogenetic activation of DS → SNr terminals produced an increase in sweetener intake that was weakened by activating SNr with CNO ($t[4] = 4.8$, $^*P = 0.0083$). CNO alone had no effect ($P = 0.60$). (**d**) Optogenetic activation of DS → SNr terminals produced a robust increase in bitter intake that was weakened by activating SNr with CNO (paired sample t test two-tailed $t[4] = 6.6$, $^*P = 0.0027$). CNO alone had no effect ($t[4] = 0.3$, $P = 0.79$). Reliable activation of hM3D(Gq)-transfected neurones in VP (**e**) and SNr (**f**) by administration of the designer drug CNO was confirmed *in vivo* using multi-channel electrophysiological recordings. Dotted line represents onset of CNO injections. Graph shows average firing rate activity over sessions. Shadowed area around trace represents s.e.m. n.s., not statistically significant. Error bars represent s.e.m.

via GABAergic mechanisms (**Supplementary Fig. 9**). We found that, in the absence of light pulses, administering the designer drug clozapine-*N*-oxide (CNO) robustly suppressed sweetener intake in both DS- and VS-implanted animals (**Fig. 4a**). Consistently, optogenetic activation of VS → VP terminals produced an increase in sweetener intake that was blocked by activating VP with CNO (**Fig. 4b**). However, activating VP with CNO produced no inhibitory effects on the robust increases in sweetener intake associated with optogenetically activating DS → SNr terminals (**Fig. 4b**). Stimulation of dorsal pathways is therefore sufficient to override suppressive commands associated with VP activation. These effects are pathway specific: when animals expressed hM3D(Gq) in SNr, CNO administration effectively inhibited increases in intake associated with optogenetic activation of DS → SNr terminals (**Fig. 4c**). Consistent with our overall model, optogenetic activation of DS → SNr terminals strongly stimulated the intake of the unpalatable bitter sugar solution, an effect that was partially blocked by CNO administration (**Fig. 4d**). Reliable activation of hM3D(Gq)-transfected neurones in VP and SNr was confirmed *in vivo* using early gene and multi-channel electrophysiological measurements (**Fig. 4e**,**f** and **Supplementary Figs. 10** and **11**). Overall, these results reveal that the dorsal DS → SNr pathway operates, to a large extent, independently of the (ventral) VS → VP pathway.

DISCUSSION

Our data imply a model for sugar reward in which hedonic and metabolic positive controls on intake are encoded and mediated by separate sensorimotor circuits (**Supplementary Fig. 12**). We found in vertebrates that the dorsal, but not ventral, basal ganglia descending pathway was recruited only when energy was present in a sweet solution. Notably, the activation of dorsal pathways was sufficient to override inhibitory signals generated by ventral pathways during the ingestion of aversive substances. Such circuit logic implemented in the striatum allows the organism to prioritize energy seeking over sensory quality.

This general trait appears to be conserved in invertebrates: *Drosophila* flies favor metabolizable over non-metabolizable sugars independently of sweet receptor activity[27]. Consistently, dopaminergic signaling mediates the ability of *Drosophila* to determine the nutritional value of sweet tastes[28], to the extent that separate dopamine neurones mediate the mnemonic encoding of gustatory and nutritional cues[29]. The separation of gustatory and post-ingestive reinforcement at the dopaminergic circuitry level therefore emerges as an evolutionary conserved trait affecting both vertebrate and invertebrates.

We found that this dopaminergic circuitry responded to intragastric infusions of sugar independently of any behavioral requirements (**Supplementary Fig. 1i**,**j**). The question thus arises of how dopamine receptor signaling may assign 'value' to the sugar stimulus. To resolve this apparent inconsistency, we first define the equivocal term value[30]. We interpret value as a stimulus property whose detection by the nervous system is sufficient to alter the probability of subsequent responding to this stimulus. The assignment of hedonic/nutritional value to the sugar stimulus is thus operationally defined by the augmenting effect of gustatory/post-ingestive signals on the probability of responding. This is functionally equivalent to the standard interpretation of value in behavioral neuroscience, in which the term refers to the motivating properties of a stimulus for instrumental action[30]. Consistently, we found that, although gut-induced dopamine release constitutes a physiological reflex, such reflex alters the probability of responding by recruiting downstream dopamine-excitable cells in striatum (**Figs. 2** and **3**). This gut-triggered mechanism thereby supports the assignment of value to sweet solutions. The same effect promptly extends to Pavlovian values[30], as demonstrated by taste-nutrient conditioning studies (**Fig. 2c**,**d**). Overall, nigrostriatal

dopamine cells may be conceptualized as sensorimotor interneurons linking physiological nutrient sensing to the assignment of value to goal-directed actions and sensory stimuli.

At least one fundamental issue remains nonetheless unaddressed. According to the model delineated above, nutritional control over intake must ultimately translate into oral-motor consummatory patterns. Our studies support a mechanism via which, following sugar intake, metabolic cues act on D1r-expressing neurones in dorsal striatum to selectively bias goal-directed action. We postulate that this is achieved via the release of brainstem oral-motor centers from tonic inhibition by SNr[25]. Our model specifically predicts that the descending pathway from SNr to the premotor reticular formation[31] links nutrient sensing in basal ganglia to the execution of feeding motor programs (**Supplementary Fig. 12**). Future research must determine the molecular identity of the circuitry that links energy sensing in forebrain to the motor central pattern generators implemented in brainstem.

METHODS

Methods and any associated references are available in the online version of the paper.

Note: Any Supplementary Information and Source Data files are available in the online version of the paper.

ACKNOWLEDGMENTS

This work was supported by US National Institutes of Health grants R01DC014859 and R01CA180030 (to I.E.d.A.), and R01 DK103176, DK084052 and NS48476 (to A.N.v.d.P.), the China Scholarship Council 201206260072 (to W.H.) and FAPESP (Sao Paulo) 2013/09405-3 (to T.L.F.).

AUTHOR CONTRIBUTIONS

I.E.d.A. conceived the study. I.E.d.A. and L.A.T. designed the experiments. L.A.T., W.H. and T.L.F. performed gastrointestinal and stereotaxic surgeries, performed behavioral and optogenetic experiments, performed microdialysis studies and analyzed data. W.H., S.J.S.-L. and T.L.F. performed histological analysis and imaging. X.Z. and A.N.v.d.P. performed whole-cell patch-clamp experiments, performed high-res imaging of brain slices and analyzed data. I.O.P. and L.A.T. performed *in vivo* electrophysiological experiments and analyzed data. I.E.d.A. wrote the manuscript. All of the authors actively participated in interpreting all data and in manuscript editing.

COMPETING FINANCIAL INTERESTS

The authors declare no competing financial interests.

1. Holman, G.L. Intragastric reinforcement effect. *J. Comp. Physiol. Psychol.* **69**, 432–441 (1969).
2. Sclafani, A. Post-ingestive positive controls of ingestive behavior. *Appetite* **36**, 79–83 (2001).
3. de Araujo, I.E. *et al.* Food reward in the absence of taste receptor signaling. *Neuron* **57**, 930–941 (2008).
4. Zuker, C.S. Food for the brain. *Cell* **161**, 9–11 (2015).
5. Stephenson-Jones, M., Kardamakis, A.A., Robertson, B. & Grillner, S. Independent circuits in the basal ganglia for the evaluation and selection of actions. *Proc. Natl. Acad. Sci. USA* **110**, E3670–E3679 (2013).
6. Everitt, B.J. & Robbins, T.W. Neural systems of reinforcement for drug addiction: from actions to habits to compulsion. *Nat. Neurosci.* **8**, 1481–1489 (2005).
7. Gerfen, C.R. & Surmeier, D.J. Modulation of striatal projection systems by dopamine. *Annu. Rev. Neurosci.* **34**, 441–466 (2011).
8. Costa, R.M. Plastic corticostriatal circuits for action learning: what's dopamine got to do with it? *Ann. NY Acad. Sci.* **1104**, 172–191 (2007).
9. Grillner, S., Robertson, B. & Stephenson-Jones, M. The evolutionary origin of the vertebrate basal ganglia and its role in action selection. *J. Physiol. (Lond.)* **591**, 5425–5431 (2013).
10. Yin, H.H., Ostlund, S.B. & Balleine, B.W. Reward-guided learning beyond dopamine in the nucleus accumbens: the integrative functions of cortico-basal ganglia networks. *Eur. J. Neurosci.* **28**, 1437–1448 (2008).
11. Wickens, J.R., Horvitz, J.C., Costa, R.M. & Killcross, S. Dopaminergic mechanisms in actions and habits. *J. Neurosci.* **27**, 8181–8183 (2007).
12. Palmiter, R.D. Dopamine signaling in the dorsal striatum is essential for motivated behaviors: lessons from dopamine-deficient mice. *Ann. NY Acad. Sci.* **1129**, 35–46 (2008).
13. Ren, X. *et al.* Nutrient selection in the absence of taste receptor signaling. *J. Neurosci.* **30**, 8012–8023 (2010).
14. Roitman, M.F., Wheeler, R.A. & Carelli, R.M. Nucleus accumbens neurons are innately tuned for rewarding and aversive taste stimuli, encode their predictors, and are linked to motor output. *Neuron* **45**, 587–597 (2005).
15. Hajnal, A. & Norgren, R. Taste pathways that mediate accumbens dopamine release by sapid sucrose. *Physiol. Behav.* **84**, 363–369 (2005).
16. Ericsson, J. *et al.* Dopamine differentially modulates the excitability of striatal neurons of the direct and indirect pathways in lamprey. *J. Neurosci.* **33**, 8045–8054 (2013).
17. Planert, H., Berger, T.K. & Silberberg, G. Membrane properties of striatal direct and indirect pathway neurons in mouse and rat slices and their modulation by dopamine. *PLoS One* **8**, e57054 (2013).
18. Yang, C.F. *et al.* Sexually dimorphic neurons in the ventromedial hypothalamus govern mating in both sexes and aggression in males. *Cell* **153**, 896–909 (2013).
19. Glendinning, J.I., Gresack, J. & Spector, A.C. A high-throughput screening procedure for identifying mice with aberrant taste and oromotor function. *Chem. Senses* **27**, 461–474 (2002).
20. Kravitz, A.V., Tye, L.D. & Kreitzer, A.C. Distinct roles for direct and indirect pathway striatal neurons in reinforcement. *Nat. Neurosci.* **15**, 816–818 (2012).
21. Lobo, M.K. *et al.* Cell type-specific loss of BDNF signaling mimics optogenetic control of cocaine reward. *Science* **330**, 385–390 (2010).
22. Cui, G. *et al.* Concurrent activation of striatal direct and indirect pathways during action initiation. *Nature* **494**, 238–242 (2013).
23. Johnson, P.M. & Kenny, P.J. Dopamine D2 receptors in addiction-like reward dysfunction and compulsive eating in obese rats. *Nat. Neurosci.* **13**, 635–641 (2010).
24. DeLong, M.R., Crutcher, M.D. & Georgopoulos, A.P. Relations between movement and single cell discharge in the substantia nigra of the behaving monkey. *J. Neurosci.* **3**, 1599–1606 (1983).
25. Wurtz, R.H. & Hikosaka, O. Role of the basal ganglia in the initiation of saccadic eye movements. *Prog. Brain Res.* **64**, 175–190 (1986).
26. Sternson, S.M. & Roth, B.L. Chemogenetic tools to interrogate brain functions. *Annu. Rev. Neurosci.* **37**, 387–407 (2014).
27. Dus, M., Min, S., Keene, A.C., Lee, G.Y. & Suh, G.S. Taste-independent detection of the caloric content of sugar in *Drosophila*. *Proc. Natl. Acad. Sci. USA* **108**, 11644–11649 (2011).
28. Burke, C.J. *et al.* Layered reward signalling through octopamine and dopamine in *Drosophila*. *Nature* **492**, 433–437 (2012).
29. Yamagata, N. *et al.* Distinct dopamine neurons mediate reward signals for short- and long-term memories. *Proc. Natl. Acad. Sci. USA* **112**, 578–583 (2015).
30. O'Doherty, J.P. The problem with value. *Neurosci. Biobehav. Rev.* **43**, 259–268 (2014).
31. Shammah-Lagnado, S.J., Costa, M.S. & Ricardo, J.A. Afferent connections of the parvocellular reticular formation: a horseradish peroxidase study in the rat. *Neuroscience* **50**, 403–425 (1992).

ONLINE METHODS

Subjects. A total of 170 adult male mice were used, including 74 C57BL6/J wild-type mice, 68 D1-dopamine receptor Cre-recombinase male mice (*Drd1a-cre*$^{+}$, strain EY262, Gensat), 12 D2-dopamine receptor Cre-recombinase mice (B6.FVB(Cg)-Tg(Drd2-cre)ER44Gsat/Mmcd, Gensat) and 16 Ai32 mice (B6.Cg-*Gt(ROSA)26Sor*$^{tm32(CAG-COP4*H134R/EYFP)Hze}$/J, Jackson Laboratory). At the time of experiments animals were 8–20 weeks old, and had no previous experiences with any of the experimental conditions. All animals were group housed (<4 cage) previous to the beginning of experimental sessions. After randomized assignment to an experimental group, all animals were housed individually. Animals were housed under a 6 a.m./6 p.m. light/dark cycle. Experiments were performed consistently between 4 p.m. and 12 a.m. to maximize motivation for feeding behavior. Each individual animal was exposed to one single experimental group. All experiments were conducted in accordance with the J.B. Pierce Laboratory and Yale University regulations on usage of animals in research.

Surgical procedures. *Gastric catheter implantation.* Once animals had been anesthetized with an intraperitoneal injection of a ketamine/xylazine (100/15 mg kg^{-1}), a midline incision was made into the abdomen. The stomach was exteriorized through the midline incision and a purse string suture was placed in its non-glandular region, into which the tip of MicroRenathane tubing (Braintree Scientific) was inserted. The purse string was tightened around the tubing, which was then tunneled subcutaneously to the dorsum via a small hole made into the abdominal muscle; a small incision to the dorsum between the shoulder plates was then made to allow for catheter exteriorization. Incisions were sutured and thoroughly disinfected and the exterior end of the catheter was plugged.

Microdialysis guiding cannulae implantation. For animals used in the microdialysis experiments, anesthesia was induced with intraperitoneal injection of a ketamine/xylazine (100/15 mg kg^{-1}) and the mouse was placed on a stereotaxic apparatus (David Kopf) under constant flow of ~1% isoflurane anesthesia (1.5 l min^{-1}). For the dorsal striatal region a circular craniotomy was drilled at AP = 1.0 mm and ML = ±1.7 mm implantation of a guide cannulae (DV = −2.0 mm from skull surface) for posterior insertion of a microdialysis probe whose exposed dialysis membrane was 2 mm high; for the ventral striatal region a circular craniotomy was drilled at AP = 1.5 mm and ML = ±0.6 mm implantation of a guide cannulae (DV = −4.0 mm from skull surface) for posterior insertion of a microdialysis probe whose exposed dialysis membrane was 1mm high.

Viral delivery of transgenes. Adeno-associated viruses (AAVs, serotype 5, University of North Carolina Vector Core) carrying genes of interest were obtained from the University of North Carolina Vector Core Services. All injections were bilateral into the structure of interest. For Cre-dependent transfection with the blue light-sensitive ion channel channelrhodopsin (ChR2), the construct AAV-EF1a-DIO-hChR2(H134R)-EYFP was used. For Cre-dependent transfection with a green light-sensitive archeorhodopsin (eArch3.0), the construct AAV-EF1a-DIO-eArch3.0-EYFP was used. For combination with chemogenetic stimulation (DREADDs), AAV-hSyn-HA-hM3D(Gq)-IRES-mCitrine was also injected in the relevant site and receptors activated by CNO at 1 mg kg^{-1} intraperitoneal. Control animals were of the corresponding strain, transfected with a light-insensitive Cre-dependent ion channel (AAV-hSyn-DIO-HA-hM3D(Gq)-IRES-mCitrine). For Cre-dependent caspase-mediated ablation of dopamine-excitable neurons in striatum, the Cre-dependent viral construct AAV-flex-taCasp3-TEVp was used. All procedures, including fiber placement and laser activation, were identical for ChR2^{+} and ChR2^{-} mice.

Caspase-mediated ablation of dopamine-excitable cells. To achieve Cre-dependent caspase-mediated ablation of dopamine-excitable neurons in striatum, the Cre-dependent viral construct AAV-flex-taCasp3-TEVp (serotype 5, University of North Carolina Vector Core) was stereotaxically injected (0.5 µl per hemisphere) into the dorsal or ventral striatum of D1r-Cre mice at same coordinates used for optogenetic experiments. The control group included non-Cre mice transfected with AAV-flex-taCasp3-TEVp. Cell-specificity of the ablations was confirmed via neuroanatomical retrograde tracing methods. The fluorescent retrograde tracer Red Retrobeads (LumaFluor) was injected into the substantia nigra, pars reticulata (0.1 µl), the exclusive ipsilateral target of D1r-expressing neurons of dorsal striatum on one hemisphere, and into the globus pallidus (0.1 µl), the exclusive ipsilateral target of D2r-expressing neurons of dorsal striatum, on the other hemisphere. It was then confirmed, using fluorescent microscopy, the strong labeling throughout dorsal striatum on the same hemisphere in which the retrograde fluorescent beads were injected into globus pallidus, and weaker labeling throughout dorsal striatum on the same hemisphere in which the retrograde fluorescent beads were injected into substantia nigra pars reticulata. Equivalent Retrobead injections were made into the ventral pallidum, the preferential target of ventral striatal D1r-expressing neurons. To allow visualization of the relevant anatomical landmarks, images show the Retrobead fluorescence signal overlaid on a bright field image of the same section.

Stereotaxic viral injections and optic fibers implantation. For animals used in the optogenetics experiments, anesthesia was induced with an intraperitoneal injection of a ketamine/xylazine (100/15 mg kg^{-1}) and the mouse was placed on a stereotaxic apparatus (David Kopf) under constant flow of ~1% isoflurane anesthesia (1.5 l min^{-1}). All viral injections were done bilateral, using modified microliter syringes (Hamilton) with a 22 needle gauge. The tip of the needle was placed at the target regions and the injections were performed at a rate of 0.1 µl min^{-1} (for coordinates and volumes see below). Once the injection was finished the needle was left in place for 10 min and then slowly removed. Immediately after the viral injection the optic fibers were implanted (200-µm core, 0.22 NA, Doric Lenses). To allow time for viral expression, animals were housed for at least 2 weeks following injection before any experiments were initiated.

Drd1a- and Drd2-cre mice were used for injections at the dorsal and ventral striatal regions. The coordinates used for dorsal striatum were AP = 1.0 mm, ML = ±1.7 mm and DV = −3.0 mm (from skull surface) and 1 µl of AAV-EF1a-DIO-hChR2(H134R)-EYFP virus was injected per hemisphere. The coordinates used for ventral striatum were AP = 1.5 mm, ML = ±0.6 and DV = −4.5 mm (from skull surface) and 0.5 µl of either the AAV-EF1a-DIO-hChR2(H134R)-EYFP or AAV-EF1a-DIO-eArch3.0-EYFP viruses was injected per hemisphere.

Ai32 mice, which express a channelrhodopsin-2/EYFP fusion protein upon exposure to Cre recombinase, were used for ChR2 expression in ventral pallidum and substantia nigra pars reticulata regions. The coordinates used for ventral pallidum were AP = 0.7 mm, ML = ±1.0 and DV = −4.9 mm (from skull surface). The coordinates used for substantia nigra reticulata were AP = −3.2 mm, ML = ±1.6 and DV = −4.4 mm (from skull surface). In both cases 0.5 µl of AAV-CMV-Cre virus was injected per hemisphere.

Drd1a-cre mice were used for the experiments involving the simultaneous activation of striatal regions (dorsal and ventral) and their downstream targets (substantia nigra pars reticulata and ventral pallidum, respectively). AAV-EF1a-DIO-hChR2(H134R)-EYFP virus was injected in the striatal regions and AAV-hSyn-HA-hM3D(Gq)-IRES-mCitrine virus was injected in the downstream targets. The coordinates and volumes employed were the same as described before for the corresponding areas.

Stereotaxic viral injections and electrode array implantation. Drd1a-cre mice were used for the extracellular recording experiments, anesthesia was induced with intraperitoneal injection of a ketamine/xylazine (100/15 mg kg^{-1}), a small incision was made into the abdominal muscle and 3 cm of MicroRenathane tubing was inserted into the intraperitoneal cavity. The purse string was tightened around the tubing, which was then tunneled subcutaneously to the dorsum via a small hole made between the shoulder plates to allow for catheter exteriorization. Immediately after, the mouse was placed on a stereotaxic apparatus (David Kopf) under constant flow of ~1% isoflurane anesthesia (1.5 l min^{-1}) for viral injections and electrode implantation. AAV-hSyn-HA-hM3D(Gq)-IRES-mCitrine virus was then injected either in substantia nigra compacta or ventral pallidum. The procedure for the virus injection was the same as described before. Once the virus injection was completed, an electrode array consisting of 16 tungsten microwires (35-µm diameter) targeting substantia nigra compacta or ventral pallidum was implanted. Locations of electrodes were confirmed histologically.

Slice electrophysiology. On the day of the experiments, Drd1a-cre mice with selective ChR2 expression in striatal D1r neurons were anesthetized with isoflurane and decapitated for electrophysiological identification of striatal D1r neurones and circuit mapping. Brains were quickly removed and immersed in an ice-cold high-sucrose solution containing (in mM): 220 sucrose, 2.5 KCl, 6 $MgCl_2$, 1 CaCl2, 1.23 NaH2PO4, 26 NaHCO3, and 10 glucose (gassed with 95% O_2/5% CO_2; 300–305 mOsm). Coronal brain slices 300 µm thick were sectioned using a vibratome. Brain slices were then transferred to an incubation chamber filled with an artificial CSF (ACSF) solution containing (in mM) 124 NaCl, 2.5 KCl, 2 $MgCl_2$, 2 $CaCl_2$, 1.23 NaH_2PO_4, 26 $NaHCO_3$ and 10 glucose (gassed

with 95% O_2/5% CO_2; 300–305 mOsm) at 22 °C. After a 1–2-h recovery period, slices containing striatum, VP or SNr were selected and transferred to a recording chamber mounted on a BX51WI upright microscope (Olympus). The recording chamber was perfused with a continuous flow of gassed ACSF. A dual-channel heat controller (Warner Instruments) was used to control the temperature of recording solution at 33 ± 1 °C. Whole-cell patch-clamp recordings were performed on striatum D1r neurons and neurons in VP and SNr that were visualized using an infrared-differential interference contrast (DIC) optical system combined with a monochrome CCD camera and a monitor. Pipettes were pulled from thin-walled borosilicate glass capillary tubes (length 75 mm, outer diameter 1.5 mm, inner diameter 1.1 mm, World Precision Instruments) using a P-97 micropipette puller (Sutter Instruments). Pipette solution containing (in mM) 145 potassium gluconate, 1 MgCl2, 10 HEPES, 1.1 EGTA, 2 Mg-ATP, 0.5 Na2-GTP and 5 sodium phosphocreatine (pH 7.3 with KOH; 290–295 mOsm) were used for whole-cell recording. The pipettes of resistances ranging from 3–6 MΩ were used for experiment. EPC-10 patch-clamp amplifier (HEKA Instruments) and PatchMaster 2.20 software (HEKA Elektronik) were used to acquire and analyze data. Pipette and cell capacitance were compensated during experiment and neurons which the series resistance was >20 MΩ and changed >15% were excluded from the statistics. Traces were processed using Igor Pro 6.36 (Wavemetrics). Inhibitory postsynaptic currents were recorded at the holding potential of −40 mV. An LED array (BXRAC2002, Bridgelux) was used to evoke the stimulation for optogenetic activation of ChR2 channels in brain slices. Continuous stimulation and stimulation of 10-ms duration with different frequency (1, 5, 10 or 20 Hz) were used in the experiment to test photostimulation-evoked response.

Stimuli and behavioral apparatus. The following taste stimuli were used as stated in the corresponding experiments: 2 mM sucralose, a mixture of 3 mM denatonium benzoate and 2 mM sucralose (sweet/bitter mixture) and 3 mM Rebaudioside A. 2 mM sucralose, and L and D-glucose solutions at a concentration of 50% (wt/vol) were used for the intra-gastric infusion coupled to oral intake experiments. All reagents were obtained from Sigma-Aldrich and prepared fresh in distilled water.

Feeding/licking experiments were conducted in either one of three identical mouse behavior chambers enclosed in a ventilated and sound-attenuating cubicle (Med Associates). Each chamber was equipped with a slot for sipper tubing placement located in the center of one of the walls and hidden by a software-controlled door, which was opened at the beginning of the sessions. From then on licking was voluntary and the animals were allowed to initiate or interrupt licking *ad libitum*. The sipper was connected to a contact-based lick detection device allowing for measurements of licking responses with 10-ms resolution. All lick timestamps were saved in a computer file for posterior analysis. Software controlled lasers and infusion pumps equipped with TTL input devices were connected to the behavioral chambers and programmed to automatically trigger laser and/or infusions in response to the detection of licks. MED-PC IV (Med Associates) was used as the platform for programming all experiments.

Behavioral sessions. Prior to obtaining the final behavioral test, animals were habituated to the behavioral boxes and the experimental conditions during five daily 1-h sessions.

Animals used for the extracellular dopamine measurements were trained to drink sucralose while receiving an intra-gastric infusion of sucralose. The exterior part of the gastric catheter was connected to a segment of MicroRenathane tubing secured to the tip of a 3-ml standard syringe containing the solutions to be infused and mounted on the syringe pump. The syringe pump was placed near a small hole made on the superior part of the sound attenuating box in such a way that mice were able to move freely inside the behavioral chambers. During the task, a detected lick triggered an intra-gastric infusion that lasted 3 s (at a rate of 0.6 ml min^{-1}, 30 µl per infusion). Licks detected while an infusion was taking place had no programmed consequences. To get the animals used to the microdialysis settings, during these sessions the mice were also connected to dummy microdialysis probes. All sessions lasted for 1 h. During the experimental session, the drinking solution and the syringe content were changed according to the different experimental conditions.

Mice exposed to the bitter-triggered intra-gastric infusions were exposed to these experimental conditions for three daily sessions before the dopamine measurements were performed (numbers of licks in each case: habituation day 1: 160 ± 22, habituation day 2: 162 ± 13, VS or DS microdialysis day (that is, day 3 or 4, counterbalanced): 118 ± 14 or 131 ± 23, repeated–measures one-way ANOVA across testing days $F[3,15] = 0.92$, $P = 0.45$. All paired t tests involving the number of licks during microdialysis versus habituation $P > 0.25$). The bitter solutions were never present in any of the intra-gastric infusates in any condition, only in solutions available for licking.

Animals used for the optogenetic experiments were first trained to drink 2 mM sucralose while plugged to the optic fibers but without receiving blue light pulses, and then later the drinking solutions and light stimulation were changed according to the different experimental conditions. To couple consumption to laser activation, detected licks triggered a 473-nm blue laser source via TTL pulses as described previously for intra-gastric infusions. Intensity at tip of fibers was estimated at approximately 5 mW. Constant pulses of light were used for D1 stimulation lasting 0.5 s, whereas 10-Hz pulses lasting 1s were used for ventral pallidum and subtantia nigra reticulata stimulation. Licks detected while the laser was on had no programmed consequences. In the D1- stimulation experiments where licking was coupled to intra-gastric infusions, the duration of the light pulses was the same than the infusions (constant light pulses lasting 3 s). All stimulations were performed bilaterally.

Conditioned taste aversion. On the first session D1-Cre mice were exposed for 30 min to a new tastant (the artificial sweetener Rebaudioside A) and 15 min after the end of the session the animals received an intraperitoneal injection of the malaise-inducing agent lithium chloride (0.35 M, 10 µl per g body weight). On the following day, conditioned aversion was tested. During this 30 min session, all groups received a 1-s light pulse per every 20 licks produced. Licks detected while the laser was on had no programmed consequences. All stimulations were performed bilaterally.

Nose poke task. Mice were placed in an operant box equipped with two slots for nose pokes at symmetrical locations on one of the cage walls. Nose pokes were connected to a photo-beam detection device allowing for measurements of responses with 10-ms resolution, and only one of them triggered the laser (1-s constant stimulation). The active side was counterbalanced among animals and responses detected while the laser was on had no programmed consequences. Two consecutive days of stimulation sessions were done and on the third day one extinction test was performed (meaning both nose pokes were inactive). All responses timestamps were saved in a computer file for posterior analysis. All experimental sessions were 30 min long. The preference ratio was calculated as follows

$$\text{Preference ratio for active side} = n(\text{active side})/[n(\text{active side}) + n(\text{inactive side})] \quad (1)$$

where n denotes the detected number of responses for the corresponding side during a given session.

Optogenetic and chemogenetic experiments. CNO was dissolved in saline to a concentration of 0.1 mg ml^{-1} and injected intraperitoneal 25 min before the beginning of the behavioral sessions. CNO was administered to each mouse (1 mg kg^{-1} body weight). During the behavioral sessions licks triggered the laser as described before (1-s constant stimulation).

To assess whether D1 stimulation had an effect on the taste perception, we performed short-term two-bottle preference tests. These experiments were carried out in a chamber equipped with two slots for sipper tubing placements, at symmetrical locations on one of the cage walls. Both sippers were connected to a contact-based lick detection device allowing for measurements of licking responses and responses produced in both sippers triggered the laser (0.5-s constant stimulation). One of the sippers contained sucralose and the other the bitter mixture. To eliminate the influence of side-biases, mice were tested for four consecutive sessions with the content of the sipper being switched across session. All sessions lasted for 10 min. Preference ratio for sucralose was calculated as described before for the nose pokes.

For intra-gastric preloads, volume was determined from the averaged infused volume across animals during habituation (~0.75 ml glucose; the same volume was used for sucralose preloads). Preload infusions were performed 10 min previous to behavioral tests, at 0.1 ml min^{-1} infusion rate. During behavioral testing, the animals were allowed to drink and self-infuse as described above. Sessions lasted for 1 h.

Nose-poking for obtaining food pellets. The same apparatus above was used in a goal-directed task in which mice were trained to poke on the active hole to obtain sugared food pellets (0.02g, BioServe). Four consecutive days of training

doi:10.1038/nn.4224

sessions were performed, after which all mice showed high preferences for the active hole (see **Supplementary Fig. 2** for details). On the fifth and sixth days the tests were performed after an intra-gastric preload infusion of glucose or sucralose. Preload volume was determined from the averaged infused volume across animals during behavioral sessions (~0.75 ml glucose; the same volume was used for sucralose preloads). Preload infusions were performed 10 min previous to behavioral tests, at 0.1 ml min^{-1} infusion rate. Sessions lasted for 1 h or 30 rewards earned, whichever occurred first.

The preference ratio for the active hole was calculated as in equation (1). Outcomes were also quantified as rewards earned for further analyses.

Brief access tests. These tests were performed to assess if cell-specific ablation of D1r-neurones in DS or VS affect hedonic responses as measured in classical brief-access tests. In these sessions, the licking spout was composed of four 20-gauge stainless-steel needles cemented together to prevent the mixing of the solutions; each needle was connected to a solenoid valve which in turn was connected to 50 mL syringes containing the solutions employed in the corresponding session. Onset of the first trial is signaled by the vertical lifting of a sliding door within the behavioral apparatus described above. Only a single sipper, located behind the sliding door, was available in these sessions. The opening/closing of one of four solenoid valves was calibrated to deliver 5-µl drops of liquid, such that taste delivery was triggered by the detected licks. Each trial lasted for 5 s from the time of the first detected lick, after which the sliding door is lowered. The taste stimuli were randomized across trials. Each session lasted for 20 min. The following variations were performed.

Tolerance to bitter. Mixtures employed were: 2 mM sucralose + 6 mM denatonium; 4 mM sucralose + 6 mM denatonium; 6 mM sucralose + 6 mM denatonium; and 8 mM sucralose + 6 mM denatonium.

Masking bitterness. Mixtures employed were: 2 mM sucralose + 6 mM denatonium; 4 mM sucralose + 6 mM denatonium; 6 mM sucralose + 6 mM denatonium; and 8 mM sucralose + 6 mM denatonium.

Sweetness. The taste stimuli employed were: 0.5 mM sucralose; 2 mM sucralose; 4 mM sucralose; and 6 mM sucralose.

Sugar-driven consumption of unpalatable solutions. To assess if cell-specific ablation of D1r-neurones in DS or VS affects the acceptance of unpalatable solutions instrumentally coupled to intra-gastric D-glucose, the following experiment was performed. Mice were exposed to bitter-triggered intra-gastric infusions of four different D-glucose concentrations (0.5, 10, 25 and 50%), each one presented in independent sessions. Glucose concentration was randomized across mice and sessions. All sessions lasted 1 h.

Taste-nutrient conditioning. First, short-term (5 min) two-bottle preference tests between sucralose and the bitter mixture were used to determine the short-term, oral relative preferences for each of these compounds before and after conditioning. To eliminate the influence of side-biases, mice were tested for two consecutive sessions with the content of the sipper being switched across sessions, and the outcome averaged. Conditioning sessions consisted of two separate 1-h one-bottle sessions. In one session, sucralose licks triggered intra-gastric infusions of sucralose. In a different session (on the next day), licks to the bitter mixture triggered intra-gastric infusions of D-glucose. The order of the conditioning sessions was counterbalanced across mice. On the following day after the second conditioning, session, the two-bottle preference tests were repeated as above. Preference ratios for sucralose were calculated as described for the nose pokes.

Open field tests. To assess locomotor activity in response to our treatments, animals were placed on a novel Plexiglas arena (Med Associates, 25 cm × 30 cm). The total area was divided into nine equal rectangular subareas (8.3 × 10 cm), demarcated with yellow tape. Immediately above the central subarea a 150-W lamp was activated to induce natural aversion to this particular location, as usually performed. Animals were tested once in this arena. The 10-min sessions were digitally recorded with a Sony HDR-CX440 camera. Data were analyzed by replaying the sessions in slow-motion. Outcomes were the number of sequential crossings over different adjacent yellow lines (representing total locomotor activity), and relative time spent within the illuminated central part of the arena. In sessions involving intra-gastric preloads, preload volume was determined from the averaged infused volume across animals during previous behavioral sessions (~0.75 ml glucose; the same volume was used for sucralose preloads). Preload infusions were performed 10 min previous to behavioral tests, at 0.1 ml min^{-1} infusion rate. In sessions involving optical stimulation, laser source was continuously on throughout the session at intermittent ON/OFF intervals of 30 s, such that a randomization was performed to determine whether the laser source would be on during any particular 30-s interval.

Control mice for optogenetics experiments. To control for genetic background, Chr2-independent light stimulation effects, and Cre-driven membrane receptor expression, D1-Cre mice were injected with the DREADD construct AAV-hSyn-HA-hM3D(Gq)-IRES-mCitrine and implanted with optical fibers exactly as ChR2-transfected mice. This thus produced Cre-dependent expression of a light-insensitive receptor in striatum. We observed that light pulses had no effects whatsoever on these animals and therefore omitted these data from main figures (where differential effects of VS versus DS stimulation are shown, thereby evidencing light-independent effects) for simplicity. For completion however we show that light pulses produced no effects whatsoever on self-stimulatory rates in control mice, in stark contrast to VS and DS ChR2+ mice in which D1-neurone self-stimulation was highly rewarding (**Supplementary Fig. 7**).

Analyses of optically triggered licking activity. Lifting vertically sliding door within the behavioral apparatus above signaled the beginning of a new trial. In each trial, the laser source was TTL-activated and left on during intervals of 1, 3, 5 or 7 s upon the detection of 13 consecutive licks to the sipper located behind the sliding door. A lick produced while laser source was on did not produce further stimulation. The length of stimulation was randomized across trials. Each trail lasted for 15 s and the timer of the trial started to run after the laser was turned on. The sessions lasted for 1 h.

Dopamine measurements during behavior. During the experimental sessions, microdialysate samples from these freely moving mice were collected, separated and quantified by HPLC coupled to electro-chemical detection methods (HPLC-ECD). Briefly, after recovery from surgery and habituation to the behavioral chambers, a microdialysis probe (CMA-7, cut off 6 kDa, CMA Microdialysis) was inserted into the striatum through the guide cannula (the corresponding CMA-7 model). After insertion, probes were connected to a syringe pump and perfused at 1.2 µl min^{-1} with artificial cerebrospinal fluid (aCSF; Harvard Apparatus). After a 40 min washout period and a subsequent 30 min pre-intake baseline sampling, dialysate samples were collected every 10 min and immediately manually injected into a HTEC-500 HPLC unit (Eicom). Analytes were then separated via an affinity column (PP-ODS, Eicom), and compounds subjected to redox reactions within an electro-chemical detection unit (amperometric DC mode, applied potential range from 0 to ~2,000 mV, 1-mV steps). Resulting chromatograms were analyzed using the software EPC-300 (Eicom), and actual sample concentrations were computed based on peak areas obtained from a 0.5 pg $µl^{-1}$ dopamine standard solution (Sigma) and expressed as percentage changes with respect to the mean dopamine concentration associated with the baseline (pre-behavioral task) sampling period. Locations of microdialysis probes were confirmed histologically.

Reverse microdialysis. Reverse microdialysis was used to perfuse DS or VS with dopamine during ingestion of sucralose or sucralose + bitter. Licks were not followed by intra-gastric infusions in these experiments. Concentrations of the perfusates were chosen based on the average baseline dopamine levels previously observed with forward microdialysis, and increased 5 times to account for dilution (DS[DA] = 1.75 ng ml^{-1} = 9.22 nM; VS[DA] = 0.6 ng ml^{-1} = 3.16 nM). Control sessions were identical except that only artificial cerebral spinal fluid (aCSF, Harvard Apparatus) was perfused. Perfusion rate was 1.5 µl min^{-1}. After a washout period of 40 min, mice were placed in the behavioral boxes while continuously perfused with aCSF. For the DA perfusion sessions, after the animal produced the first 20 licks, the aCSF perfusate was switched to aCSF+DA. On these sessions samples were collected every 10 min and analyzed as described before to confirm that the reverse microdialysis was effective.

Electrophysiological recordings and firing rate analysis. Neural electrical activity was recorded from a movable 2 × 8 array of 16 tungsten microwires using a multichannel acquisition processor (Tucker-Davis Technologies). Only single neurons with action potentials of signal-to-noise ratios >3:1 were analyzed. The action potentials were isolated online by means of voltage-time threshold windows and a three-principal components contour templates algorithm. Spikes were resorted using Offline Sorter software (Plexon). Data was then imported into

Matlab for analysis using custom-written software. To calculate the firing rate, instantaneous firing rate was smoothed using Matlab smooth with a 60-s moving average. To test the significance of firing rate changes, we used an individual unit analysis. A one-factor ANOVA was performed on each unit to determine whether the mean firing rate after the intraperitoneal injection (of either saline or CNO) was significantly different from that before the injection (baseline) and units were classified in three populations: excited, inhibited and neutral. Finally, an odd-ratio test was performed on those population to determine the change in ratios (CNO:SAL). All recordings were performed in the home cages and the intraperitoneal catheter was used to deliver the intraperitoneal injections. The exterior part of the intraperitoneal catheter was connected to a segment of MicroRenathane tubing secured to the tip of a 1-ml standard syringe containing the solutions to be injected and mounted on the syringe pump. The syringe pump was placed on top of the cage in such a way that mice were able to move freely inside the home cage. The CNO dose was the same used for the behavioral experiments (1 mg kg^{-1}). The rate of the injections was calculated in such a way that all injections lasted for 1 min.

Histological analyses. Mice were killed with a lethal dose of ketamine and xylazine (400 mg ketamine + 20 mg xylazine kg $body^{-1}$ intraperitoneal). All animals were transcardially perfused with filtered saline, followed by 4% paraformaldehyde (wt/vol). Following perfusion, brains were left in 4% paraformaldehyde for 24 h and then moved to a 20% sucrose solution (wt/vol) in phosphate-buffered saline (PBS) for 2 d. Brains were then frozen and cut into four series 40-µm sections (either coronal or sagittal) with a sliding microtome equipped with a freezing stage. To identify fiber and electrode locations, relevant sections were identified and mounted on slides. Sections were then photographed under bright field and fluorescence. For c-fos measurements, unilateral stimulation was performed using 1 min ON/1 min OFF cycles during 10 min. For striatal stimulation 0.5-s on/0.5-s off cycles were used during the ON cycles, and 10 Hz was used for pallidum and substantia nigra stimulation. 90 min after the stimulation protocols mice were sacrificed and perfused as described before.

Fos expression analyses. To visualize Fos immunoreactivity, we used the ABC/DAB procedure. Briefly, brain sections were first rinsed with 0.02 M potassium phosphate buffer (KPBS, pH 7.4), then immersed into a incubating solution (2% normal goat serum (NGS, vol/vol) and 0.3% Triton X-100 (vol/vol) in KPBS) containing a rabbit polyclonal antiserum directed against the N-terminal region of the Fos gene (Ab-5, Calbiochem; dilution 1:10,000) and incubated at 4 °C for 36 h. After primary antibody incubation, tissues were washed in 0.02 M KPBS and incubated at 22 °C for 2h with goat anti-rabbit, biotinylated secondary IgG (anti-rabbit IgG, Vector Laboratories, 1:200), washed again in 0.02 M KPBS and subsequently reacted for 1 h with avidin-biotin-peroxidase complex (ABC method, Vectastain Elite ABC kit, Vector Co.) at 22 °C. A nickel diaminobenzidine (Nickel-DAB) glucose oxidase reaction was used to visualize Fos-like immunoreactive cells. Finally, sections were washed in KPBS and mounted, air-dried, dehydrated in alcohol, cleared in xylene, and coverslipped.

Fos expression was analyzed and quantified as follows: coronal sections at ~160-µm intervals throughout the rostral-caudal extent of the ventral pallidum and the substantia nigra reticulata were photographed at 10× magnification and montaged with Adobe Photoshop to preserve anatomical landmarks. Fos+ neurons were counted manually on each slice (five slices per animal for ventral pallidum and seven slices per animal for substantia nigra reticulata) and expressed as the cumulative sum of Fos+ neurons within the relevant regions for each animal.

Overall experimental design and analysis. *Overall design.* Data collection and analysis were not performed blind to the conditions of the experiments, due to the nature of most experiments (stereotaxic position of microdialysis probe, laser state ON versus OFF). Data were collected and processed as blocks according to the experimental conditions. Animals were randomly assigned to the different experimental groups.

Exclusion criteria. No animals that completed the appropriate experimental condition, or any associated data points, were removed from the final analyses. A priori criteria determined that animals showing post-surgical signs of distress or excess weight loss were removed before the completion of the studies. For optogenetic experiments, a priori exclusion criteria related to lack of expression of Cre-dependent ChR2 in striatal neurons. One entire group of animals ($N = 6$) was replaced due to lack of $ChR2^{+}$ expression in any striatal neuron.

Sample sizes. Samples sizes were determined based on our own previous studies employing similar neurochemical, optogenetic and behavioral approaches. Samples sizes adopted in our current study were sufficient for detecting robust effect sizes while complying with guidelines enforcing minimal animal usage and distress.

Statistical analyses. Data analyses were performed using SPSS (PASW Statistics Release 18.0.0) and Matlab (v.14a, MathWorks). Data distribution was assumed to be normal but this was not formally tested due to normality tests being inconclusive when small sample sizes are employed (normal probability plots instead). Consistently with the overall experimental design and group assignments, statistical analyses only made use of standard linear model (Pearson correlation) analyses as well as one- or two-way (repeated measures) ANOVAs and *post hoc t* tests whenever relevant. All *P* values associated with the *t* tests performed correspond to two-tailed tests, and all *post hoc* tests were corrected for multiple comparisons by employing Bonferroni correction. All data are reported as mean ± s.e.m. Every experimental group entered in statistical analyses was associated with the corresponding computation of its mean ± s.e.m.

Code availability. MED-PC IV (Med Associates) was used as the platform for programming all experimental schedules involving behavioral and optogenetic protocols. All custom codes employed to generate behavioral and optogenetic data are freely available upon request.

A **Supplementary Methods Checklist** is available.

doi:10.1038/nn.4224